386

Tropical cyclone forecasting at ECMWF: new products and validation

Gerald van der Grijn

Operations Department

September 2002

For additional copies please contact

The Library
ECMWF
Shinfield Park
Reading, Berks RG2 9AX

library@ecmwf.int

Series: ECMWF Technical Memoranda

A full list of ECMWF Publications can be found on our web site under:
http://www.ecmwf.int/publications.html

1 Introduction

In recent years ECMWF has increased its focus on severe weather prediction and work has also been done to improve the model performance in the tropics, specifically concerning tropical cyclones (TCs). The aim was to improve the skill of TC forecasts and to reduce the downstream development of forecast errors when TCs enter the mid-latitudes. From 22 January 2002, tropical perturbations were added to the initial perturbations of the ECMWF Ensemble Prediction System (EPS).

In the past, adiabatic singular vector (SV) perturbations were applied only in the mid-latitudes. Barkmeijer et al. (2001) and Puri et al. (2001) found that to benefit from SV perturbations in TC ensemble forecasting, it was necessary to define target areas in the vicinity of TC locations rather than using the entire tropical region and to ignore perturbation growth above 500hPa in a diabatic SV computation. A more recent study regarding the impact of these so-called "targeted tropical singular vectors" on ensemble TC tracks is presented in Palmer et al. (2001).

On the same date, the use of QuikSCAT data in the data assimilation was introduced. The QuikSCAT sea surface wind observations were expected to give valuable information in data scarce areas over the oceans and, therefore, improve the model's analysis and subsequent forecast, in particular with respect to TCs.

To assess the skill of the model with respect to TCs several tools and forecast products have been developed. The TC tracker is the essential tool for TC forecasting and subsequent verification. The tracking algorithm is discussed in section 2. Some recently developed TC forecast products are discussed in section 3. Section 4 deals with the TC verification scores.

2 ECMWF tropical cyclone tracker

Over the past decades several meteorological centres have developed their own tracking algorithm for TCs or mid-latitude cyclones. Although WMO standards for cyclone tracking are lacking, there are some basic principles that are applied in most tracking algorithms. Mean sea level pressure (MSLP) or vorticity (VORT) is usually used to determine a cyclonic centre. The search for the TC centre is usually done in a box or radius around a "first-guess" location. The first-guess location is often obtained by extrapolating past track positions or by advection of the TC with the steering current. The size of the search area is an essential parameter in the tracker. The risk of tracking a synoptic feature that has nothing to do with the initial TC increases with a larger search area. Therefore, care must be taken to ensure that the TC centre that is found not only resembles a TC, but is also the TC that is being targeted. Vitart and Stockdale (2001) describe a TC tracker used for the ECMWF Seasonal Forecasting System. Apart from a minimum in MSLP and a maximum in VORT, their tracker also requires a warm core before a TC can be defined as such. The U.K. Met. Office (UKMO) tracker (Heming, 1994) uses cyclonic vorticity to define the centre of a TC. The NCEP hurricane tracker (Marchok, 2002) however, defines a TC using more than one meteorological parameter (MSLP, 700 and 850 hPa vorticity, 700 and 850 geopotential height, 700 and 850 hPa wind). A description of the so-called "enhanced FNMOC tracker" can be found in Fiorino (2002). This tracker is primarily based on surface wind speed in determining TC centres. Sinclair (1994) describes a tracking algorithm for cyclones in the southern hemisphere (not necessarily TCs).

2.1 Input data

2.1.1 Tropical cyclone observations

TC observations are a vital part in the ECMWF tracker. A TC will only be tracked in the 12UTC model run if there is at least one observation of that TC available in a 6-hour window around the analysis time. In other

words, the tracking algorithm does not take TC genesis into account - i.e. the forecast development of a TC initiated from an analysis where no TC was present.

TC observations are received from various regional centres around the world such as the Joint Typhoon Warning Centre in Hawaii and the National Hurricane Centre in Miami. The regional centres are responsible for issuing warnings and advisories for TCs that are present in their basin. The reports are usually issued every six hours for each active TC and include information about the estimated location, direction of movement, maximum winds and core pressure of the cyclone.

Some centres issue "best track" observations for each storm in their area of responsibility. It must be noted that these best tracks may differ from the real time observations received at ECMWF because of additional information becoming available after the issue of the advisory such as satellite or aircraft observations.

2.1.2 Model fields

In principle the tracker can run with any model resolution. The algorithm currently in use at ECMWF uses model data on a 0.5° by 0.5° cylindrical equidistant (lat-lon) grid. Starting from the analysis, TCs are tracked until the 5-day forecast (+120h). The tracking is done with a 12-hour time resolution for the EPS and a 6-hour time resolution for the high-resolution deterministic model.

2.2 Tracking algorithm

The tracking algorithm currently in use at ECMWF is based on extrapolation of past movement, the mid-troposphere steering flow (V_{av}). The steering flow and the previous displacement vector are used to calculate the first guess position of the next tracking point.

The dominant influence on TC movement is the large-scale steering flow. However, determination of the steering flow for a given TC is not unique and many different levels and layers have been proposed for use. Generally, more intense storms extend higher in the troposphere and have higher steering levels (Dong and Neumann, 1986). The steering flow in the ECMWF TC tracker is a layer average of the 850hPa, 700hPa and 500hPa wind. To separate the TC wind field from the large-scale environmental wind fields a very low T20 spectral resolution is used.

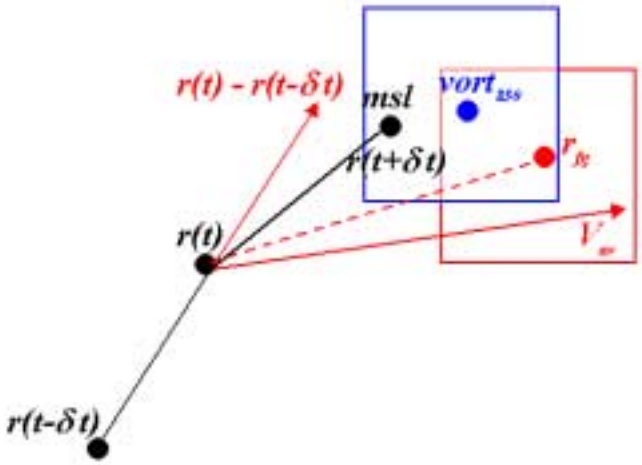

Figure 1: Schematic overview of ECMWF tracking algorithm

If a TC is verified in the analysis it will be tracked in subsequent forecasts. Fig. 1 gives a graphical representation of the tracking algorithm. At forecast time t, a TC is present at $r(t)$. The first guess position vector for the next-track position r_{fg} at time $t+\delta t$ is based on a weighted combination of the previous displacement, $r(t)-r(t-\delta t)$, and the steering flow, V_{av}, and can be written as (adaptation from Sinclair, 1994):

$$r_{fg}(t+\delta t) = r(t) + w_m[r(t) - r(t-\delta t)] + (1-w_m)V_{av}\delta t \quad (1)$$

w_m is a weight and has a value between 0 and 1. The choice of w_m is a measure of the degree of reliance on the past motion: the shorter δt, the closer w_m will be set to 1. In the ECMWF TC tracker, w_m is set to $\frac{1}{3}$ when using EPS fields (12h forecast steps) and w_m is equal to α $\frac{1}{2}$ when using high-resolution deterministic fields (6h forecast steps).

When the first guess (r_{fg}) of the next track position has been calculated, a search is made for the maximum (or minimum on southern hemisphere) of $VORT_{850}$ in a 7° by 7° box centred on r_{fg}. A similar box is then applied around the $VORT_{850}$ extreme in which a search is made for the minimum in MSLP. Finally, the position of this gridded MSLP minimum is interpolated to a sub-grid location using the scheme that is presented in the appendix. The location of the MSLP minimum becomes the next track point, $r_{t+\delta t}$.

The tracker stops if one (or more) of the following conditions is met:

- The centre of a TC is not between 45°S and 45°N.
- The absolute value of the $VORT_{850}$ extreme is below $7x10^{-5}s^{-1}$
- The value of the MSLP minimum is above 1010hPa.

If for any reason the tracker stops before reaching the maximum forecast step (t+120), a flag is put in the tracker output representing the reason for the cancellation of the tracker.

3 Tropical cyclone forecast guidance

The concept of probability forecasting is important when dealing with severe weather prediction. A forecaster is not necessarily interested in the best possible estimation of future weather. The severest and often less likely scenarios need most attention in severe weather prediction.

Conventional probability maps are useful in assessing the likelihood of a certain event at a specific location. Fig. 2 shows a wind probability map related to TC 11S, also known as Hary. A drawback of such a probability map is that probability values do not always “add up”. In theory, probability values can be very low even when all EPS members support a specific event (e.g. 10m wind speed exceeding 25 m/s). For example, probabilities will not be higher than 2% if all 50 EPS members predict the event but all at different grid points or at different time steps.

The information obtained by the tracker can be used as a basis for a different type of probability map.

3.1 Strike probability

The tracker generates 50 perturbed plus 1 unperturbed control track (CTRL). From these tracks it is possible to calculate the probability that a TC will be at a certain location at a certain time. However, note that a forecaster is often more interested in *whether* a TC will affect a certain area than *when* that TC will hit a specific location; the *exact* location of the TC is of less importance.

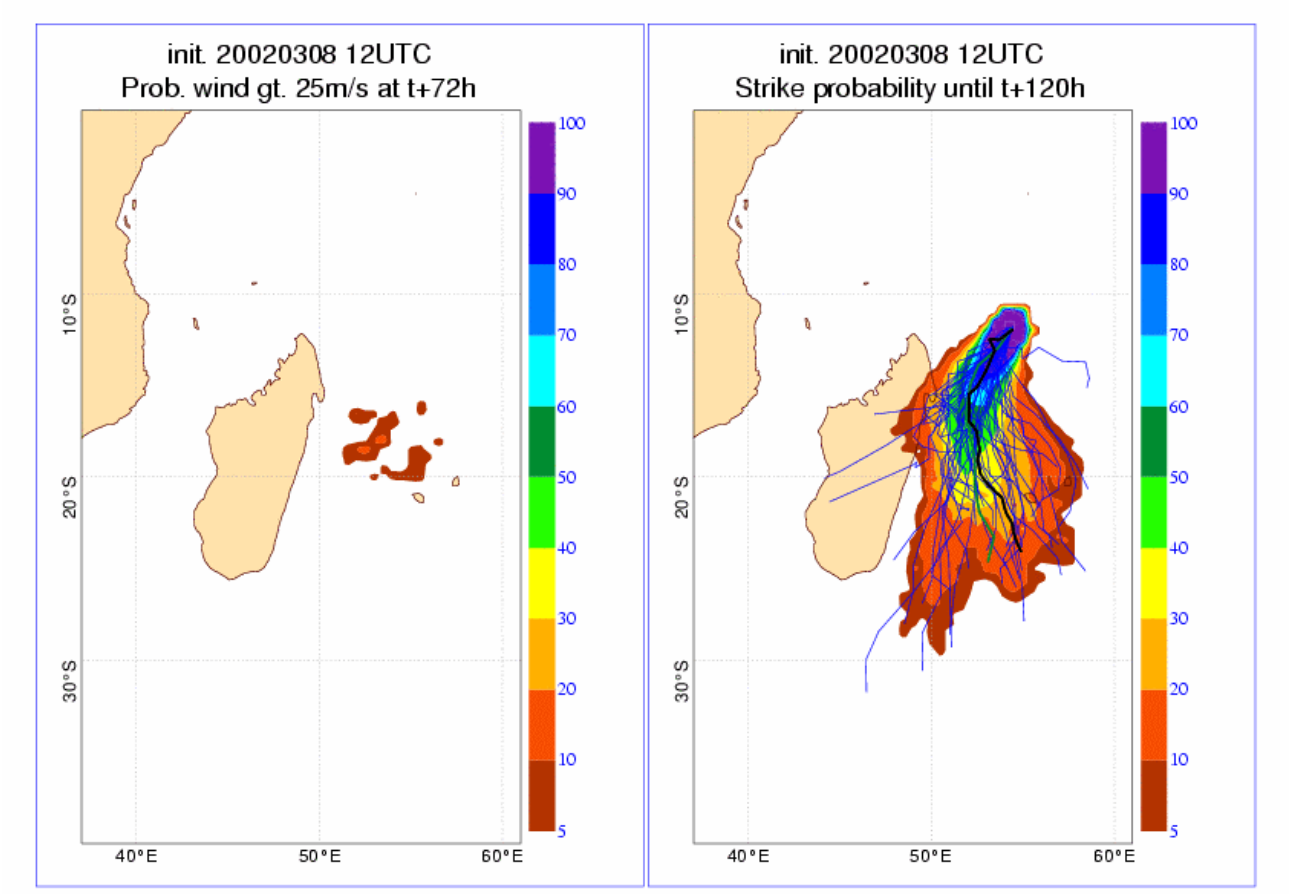

Figure 2: Conventional probability map (left tile) shows the probability that the 10m wind exceeds 25m/s at t+72h in the area of TC 11S; strike probability of TC 11S (right tile) is based on 51 EPS tracks (50 members (blue) + 1 CTRL (green)); the track of the high-resolution deterministic model (OPER) is shown in black

The concept of "strike probability" originates from this idea. The strike probability is defined as "the probability that a TC will pass within a 65nm radius from a given location at anytime during the next 120 hours". The strike probability is based on the number of members that predict this event, each member having an equal weight. The actual value of 65nm corresponds roughly with the value that is in use at the National Hurricane Center (NHC) in Miami (USA).

An advantage of a strike probability map as presented in Fig. 2 is the elimination of the time dimension. It allows the user to make a quick assessment of the high-risk areas regardless of the exact timing of the event. Another feature of a strike probability map is that it gives the forecaster an estimate of the skill that can be expected from the CTRL. This is because on average the CTRL track error should be equal to the ensemble track spread. In other words, the width of the probability plume is a direct measure of the spread in the EPS and would ideally be a good indicator of the expected error in the CTRL (Buizza, 1997). Elsberry and Carr (2000) also found that a small spread in TC tracks of 5 different models is often indicative of a small consensus track error.

As mentioned earlier, a strike probability map does not give clear guidance about the timing of the event. It also does not give any information about the strength of the TC in terms of wind speed. A strike probability map should therefore always be used in conjunction with other forecast guidance tools.

3.2 Langrangian time series

Contrary to a strike probability map, which highlights risk areas at the cost of discarding the time dimension and TC intensity information, a "Langrangian time series" (LTS) is able to highlight the distribution of meteorological parameters like TC core pressure and 10m-wind speed. An LTS shows the EPS distribution associated with a meteorological feature, in this case a TC, rather than the EPS distribution at a certain grid point. In other words, the user of an LTS is focused on the feature rather than the grid point. Instead of determining the EPS distribution at a specific grid point, as it is usually done in conventional probability maps, it determines the EPS distribution in a 7° by 7° box centred on a TC location.

Fig. 3 shows an LTS for tropical cyclone 11S, based on the same model base date as Fig. 2. Fig. 2 suggests that not more than 20% of the EPS members predict wind speeds exceeding 25m/s at t+72. However, the LTS produced with the tracker shows that at this forecast step at least 50% of the EPS members have wind speeds exceeding this threshold.

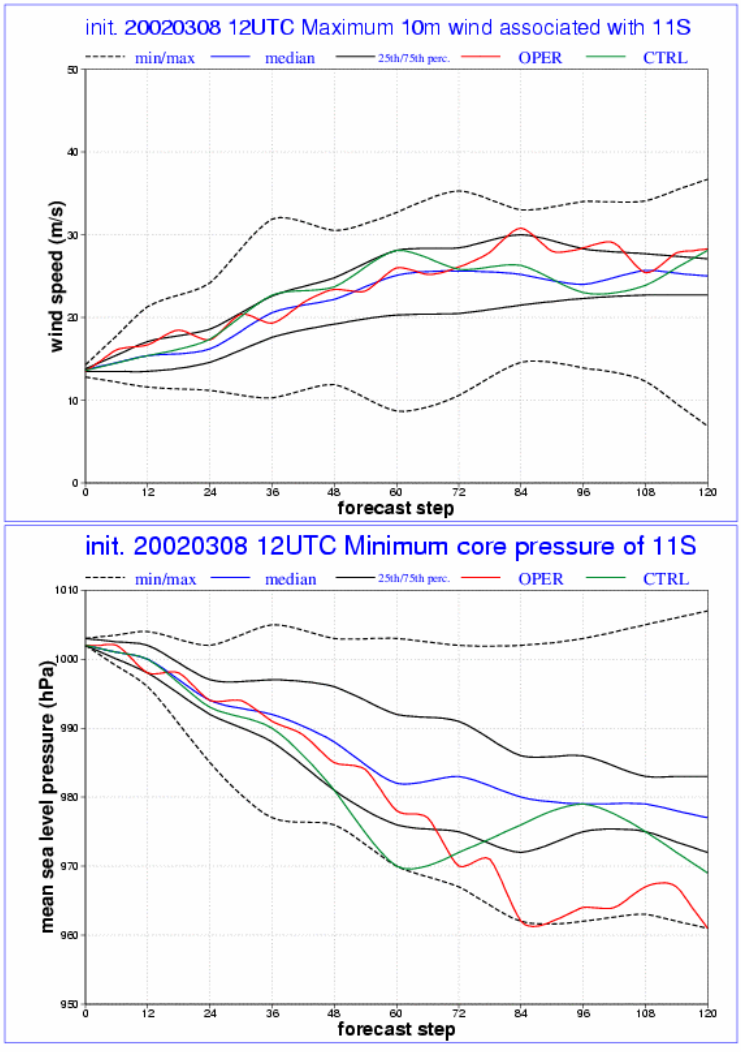

Figure 3: Langrangian time series of TC 11S for maximum 10m-wind speed (upper tile) and minimum core pressure (lower tile); EPS distribution: min/max (dashed), 25th/75th percentile (solid black) and median (blue); OPER and CTRL area shown in red and green respectively; the smoothed curves are based on 6-hourly data for OPER and 12-hourly data for the EPS

4 Evaluating tropical cyclone forecast skill

As mentioned already earlier, the introduction of QuikSCAT data into the data assimilation was expected to have a positive impact on the model's capability of analysing TCs. Furthermore, the change in the EPS by adding targeted tropical SV was expected to increase the skill of the EPS with respect to TCs, therefore showing a better estimate of forecast uncertainty.

Both model changes have led to the development of a tool, the ECMWF TC tracker, that would make objective verification of TC track forecasts possible.

4.1 QuikSCAT and deterministic forecast skill

The use of QuikSCAT data in the data assimilation was introduced in model cycle 24R3 in January 2002. In order to evaluate the increase in skill, a comparison was made with the previous two model cycles 23R4 and 23R3.

Model cycle 24R3 was run in parallel with 23R4 and 23R3 for the first two weeks of September 2001. The statistics are based on a homogeneous sample containing 56 forecasted cyclone tracks representing 11 independent TCs. A cyclone had to be successfully tracked in all three model cycles in order to be included in the sample. In other words, for each forecast step the sample contains only those TCs that are detected in all model cycles.

Fig. 4 shows the mean core pressure error and positional error for different forecast steps up to t+96. A gradual improvement of skill can be seen with model upgrades. However, despite this increase in skill there is still a large positive bias in core pressure to be seen. The reason for this is that global atmospheric models are simply not (yet) designed to resolve the extreme pressure gradients associated with TCs. The bias is around 18hPa in the analysis and increases to around 25hPa at t+72. The bias seems to decrease, or at least to saturate, later in the forecast. Apparently the model is more capable in developing TCs with a realistic core pressure in the forecast than analysing them in the initial conditions. This surprising result might come from either an analysis being too smooth, possibly because of the reduce resolution (T159) of the minimisation increments, or an over development of TCs in the model, possibly because of a crude representation of the physics or of the interaction with the ocean.

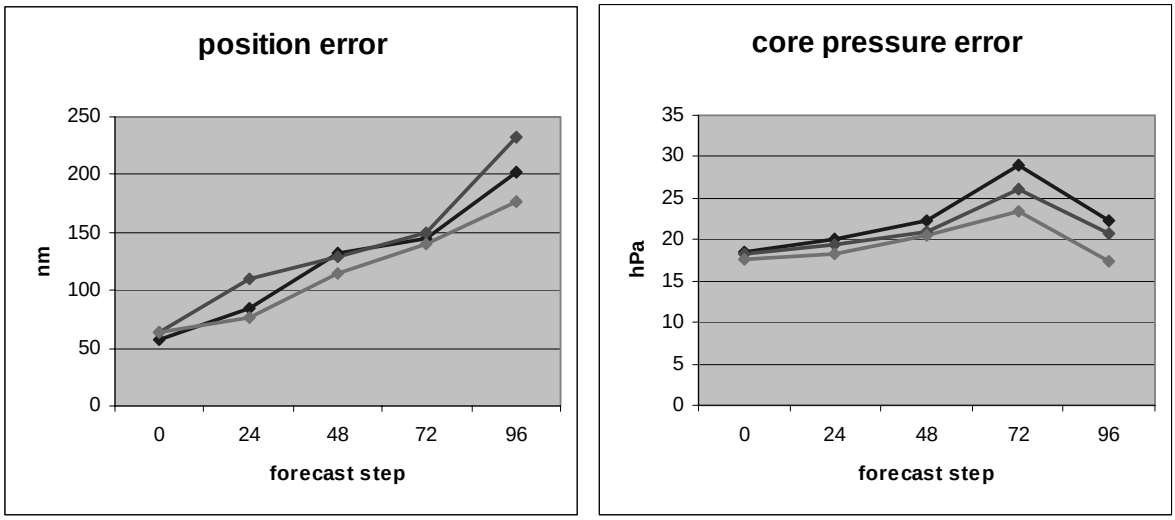

Figure 4: Core pressure error and position error for different forecast steps (in hours) and model cycles, 23R3 (blue), 23R4 (red) and 24R3 (green); sample taken from 2001-09-01 until 2001-09-14

The positional error amounts to around 60nm in the analysis and 111nm at t+48 in the most recent model cycle. These values compare to 20nm and 126nm resp. for UKMO (U.K. Met Office, 2001).

The large difference in positional error in the analysis between ECMWF and UKMO is probably due to the fact that UKMO uses a "TC bogusing" technique in their analysis. In addition, a different tracking algorithm than described in section 2 was used in gathering these statistics. The ECMWF TC tracker used for Fig. 4 determined the cyclonic centre on the basis of the $VORT_{850}$ extreme rather than the MSLP minimum as described in section 2. In most cases the centre of a TC as defined by $VORT_{850}$ will not differ greatly from that defined by MSLP. In some cases however, when the TC is very asymmetric, the two methods will produce considerably different results. It should be noted as well that the UKMO statistics mentioned above are based on September 2001 whereas the ECMWF sample contains only the first two weeks of that month.

4.2 Targeted tropical singular vectors and ensemble forecast skill

The implementation of model cycle 24R3 also included the introduction of targeted tropical SVs in the EPS. To evaluate the impact on probabilistic TC forecasts, 24R3 was run in parallel with (at that time operational) model cycle 23R4, both in EPS mode. The parallel run was done for two periods: 1 September 2001 until 14

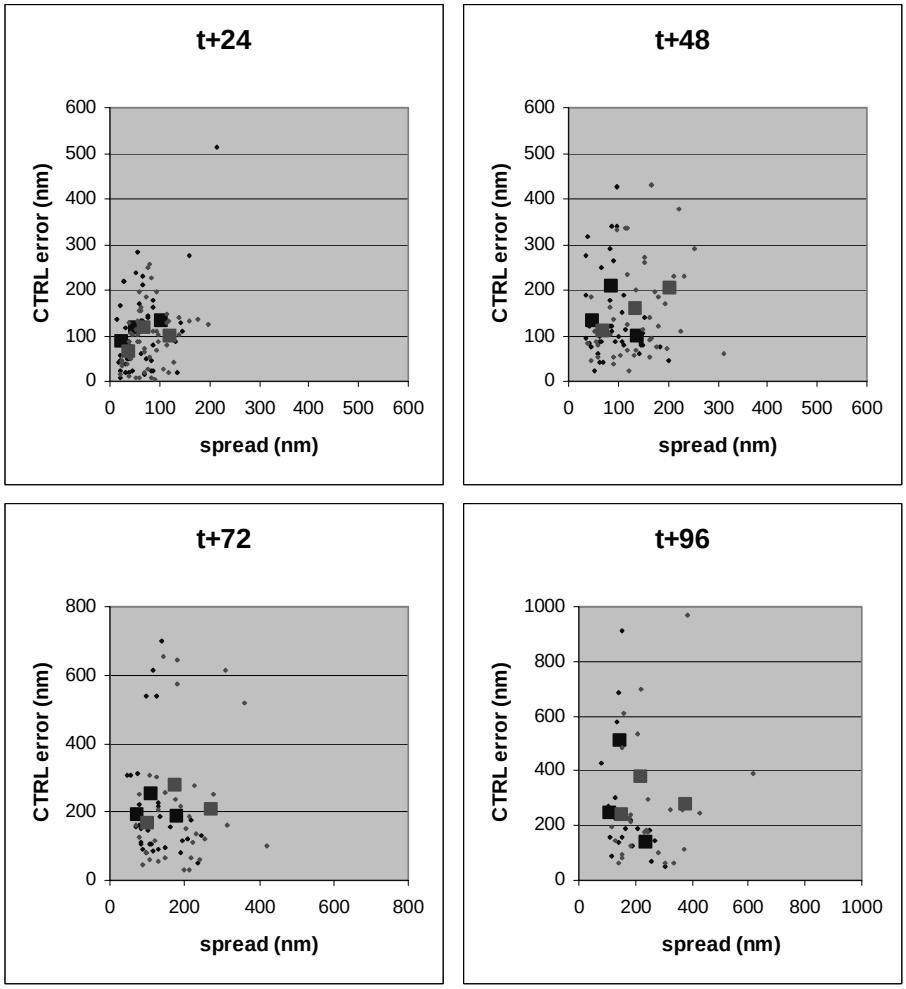

Figure 5: EPS spread versus CTRL error for model cycles 23R4 (blue) and 24R3 (red) for different forecast steps; to provide an estimate of the conditional mean error, the sample has been divided into equally sized bins (squares)

September 2001 and 20 October 2001 until 6 November 2001. For convenience this period will be referred to as SON 2001. During SON 2001 there were 86 probabilistic forecasts representing 17 different TCs.

Figure 5 illustrates the spread-skill relationship for 23R4 and 24R3 for different steps. The spread is defined as the standard deviation of the distance between the ensemble tracks and the mean ensemble track. Skill is measured by the distance error between the CTRL track and observed TC positions. Ideally, the spread would be a good indicator of the CTRL skill, which would result in points close to the unit line in Fig. 5.

For most forecast steps model cycle 24R3 shows a better correlation between spread and skill than 23R4. Especially at t+24 and t+48 a low spread in 24R3 is on average followed by a small CTRL error. At t+72 and t+96 the picture is not so clear anymore. More verification results are needed in order to determine whether the weak spread-skill relationship at t+72 and t+96 is due to the EPS itself or simply a sample size artefact.

An important aspect of a probabilistic forecast system is its reliability. The reliability measures the ability of the system to forecast accurate probabilities. In other words, does a 60% probability really mean that the event will verify on average in 60 cases out of 100. Using a perfect forecast system and a large sample of forecasts, a 20% forecast probability will only verify in 20% of those cases.

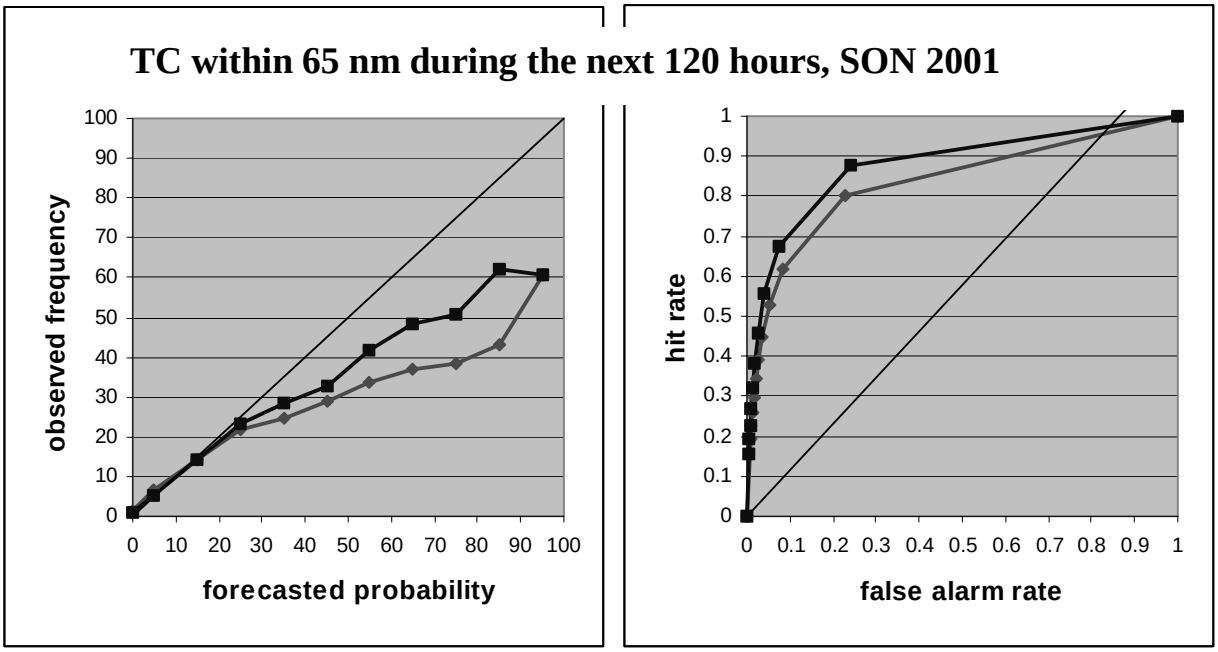

Figure 6: Reliability diagram (left) and ROC (right) for the forecast probability that a TC will pass within 65nm anytime during the first 120 hours of the forecast; red lines: cycle 23R4, blue lines: cycle 24R3; each point on the ROC corresponds to a different threshold: from top-right to bottom-left these are 0%, >0%, >10%, >20%, …, >90% and 100%

In a so-called reliability diagram this would result in points lying on the unit line. Fig. 5 shows the reliability diagram for the strike probability (event of a TC passing within 65 nm radius during the next 120 hours). A clear improvement in reliability can be seen in 24R3 over 23R4. However, the system is over-confident in the high probability range. A 95% probability forecast only verifies in 60% of the cases. This might be an indication that the spread is still a bit too low in the early forecast steps.

Another convenient way to summarize the skill of a probabilistic forecast system that can be adjusted by the user's requirement with a variable decision-making parameter is by computing Relative Operating

Characteristics (ROC) curves. If the probabilistic forecast system is the EPS TC tracks, then the decision-making parameter can be the strike probability. For each strike probability threshold, a contingency table can be made containing the number h of "hits" (event forecasted and observed), f of "false alarms" (event forecasted but not observed), m of "missed events" (event not forecasted but observed) and z of "zeros" (event not forecasted and not observed). Each point on the ROC curve corresponds to a different threshold of the strike probability. The closer the ROC lies to the ideal point of (0,1), which means that no false alarms for the event are given and no event is missed, the better the skill of the forecast system. The right panel in Fig. 5 shows the ROC curves for the strike probability for 23R4 and 24R3. Just like the reliability diagram (left panel) a clear improvement of 24R3 over 23R4 can be seen. It must be noted that despite the small values of the false alarm rate (FAR), the actual number of false alarms is quite large. The FAR in a ROC diagram is defined as the number of false alarms per "No" event ($\frac{f}{f+z}$). In severe weather forecasting the value of z is usually very high ($z >> h$). The more commonly used false alarms per "Yes" forecast ($\frac{f}{f+h}$) turns out to be much larger. However, taken the severity of the event into account and the loss involved, it is likely that most users will favour a forecast system that is designed to reduce the number of misses at the expense of a higher amount of false alarms.

4.3 Tropical cyclone forecast skill during FMAM 2002

4.3.1 Deterministic verification

The scores for verifying deterministic TC forecasts as presented in section 4.1 are quite limited. The position error, for example, gives an indication of how well a TC track was forecast but gives no information as to whether the forecast errors were resulting from a slow or fast bias in the forecast track or maybe from a tendency to steer pole wards too soon. Error scores that do address these issues are commonly used in TC verification and are known as the along-track error (ATE) and cross-track error (CTE). An explanation of these errors can be found in Fig. 7.

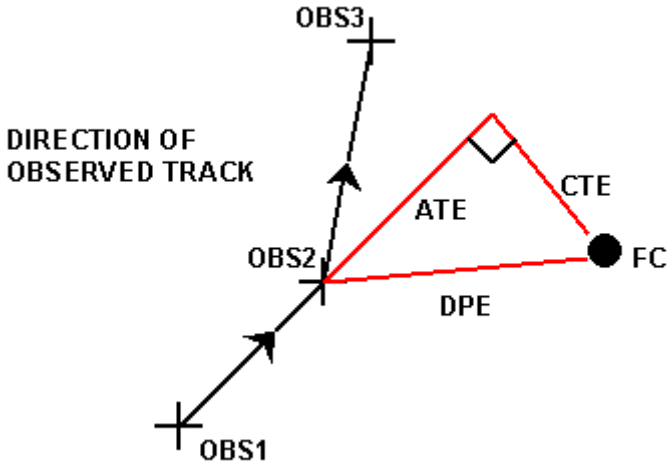

Figure 7: Diagrammatic explanation of direct position error (DPE), cross-track error (CTE) and along-track error (ATE). In this example, the forecast position is ahead and to the right of the verifying observed position (OBS2). Therefore, the ATE is positive (ahead or faster than the observed track) and the CTE is positive (to the right of the best track). The ATE and CTE should be examined together and they are not always conclusive. For example, a very large CTE will result in an ATE that indicates a slow bias, even if the TC has the correct speed. Adapted from Heming (1994).

The skill of the deterministic TC forecasts has been assessed for FMAM 2002. Apart from an assessment of the positional error statistics explained in Fig. 7, the skill of the forecasted intensity of the TC has also been evaluated. The results are shown in Fig. 8. A noticeable feature of Fig. 8 is the rapid decrease in sample size with increasing forecast step. The ECMWF tracker detected just over 80 TCs in the analysis whereas this value has dropped to just below 20 for a D+5 forecast. Some decline in sample size, however, *should* be seen. A TC that is observed in real-time and detected in the analysis can dissipate or become extra-tropical a few days later. This natural and unavoidable decline in sample size is depicted with the green curve. It shows the optimum sample size if the model and the ECMWF tracker were to be 100% perfect. However, there are instances that for various reasons the ECMWF tracker fails to detect a TC or that a TC is forecasted to dissipate while it is still observed in real-time at the verifying time. The distance between the green and the red/blue curve represents this undesirable decline in sample size. The ratio is also known as the detection rate.

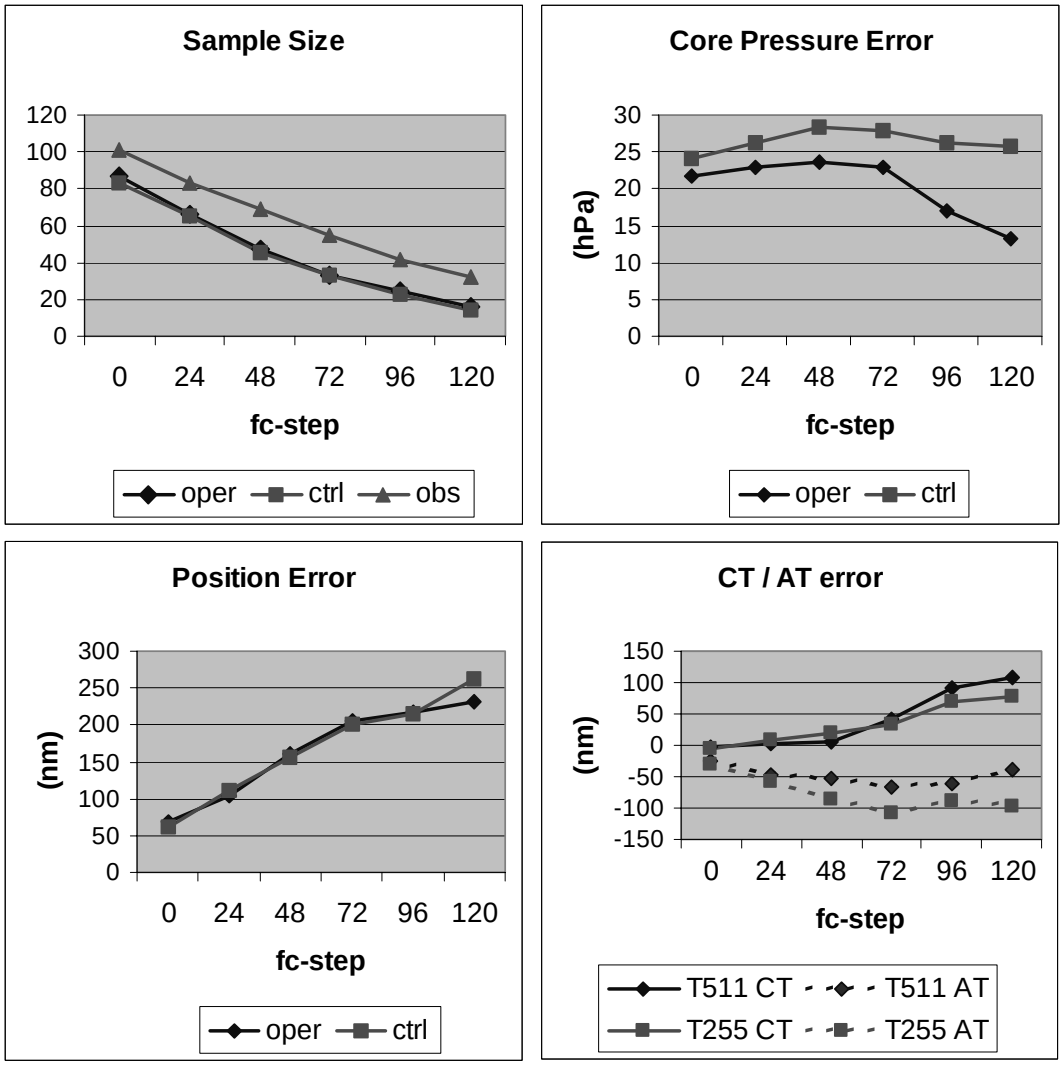

Figure 8: Forecast errors and sample sizes at different forecast steps during February, March, April and May (FMAM) for the high resolution T511 (OPER) and the lower resolution T255 EPS control (CTRL).

The forecast error in core pressure is always positive which means that the TCs in the analysis and forecasts are on average weaker than observed. This is especially the case for the lower resolution CTRL. Just as in

Fig. 4, saturation in core pressure error can be seen with increasing forecast step. However, the absolute values of the core pressure error in the early forecast steps are higher in FMAM 2002 than in September 2001. This difference might be a result from the smaller sample used for Fig. 4. However, it may also be that the skill of TC intensity forecast is basin dependent. The sample for September 2001 contains only northern hemispheric TCs whereas the FMAM 2002 sample consists mainly of southern hemispheric TCs.

The DPE amounts around 60nm in the analysis and increases almost linearly to around 250nm at D+5. Model resolution does not seem to have much impact on the DPE. The bottom-right plot in Fig. 8 shows that both OPER and CTRL have a slow and right-off track bias. However, in this case model resolution seems to play a role. From analysis until D+3 forecast, the ATE for CTRL is almost twice as large as for the OPER while having a comparable CTE. The decreasing negative bias in the ATE after D+3 is not necessarily a result from the increase in the TC speed but may as well, as explained earlier, be caused by a large value of the CTE.

4.3.2 Probabilistic verification

The performance of the EPS has also been evaluated for FMAM 2002. Fig. 9 shows the resulting reliability and ROC diagrams. The reliability diagram reveals that the system is clearly over-confident, even more than for SON 2001 (Fig. 6). Again, this difference might be due to the difference in TC basins during those periods. The same applies to the ROC diagram, which is slightly worse for FMAM 2002 than the ROC curve based on SON 2001.

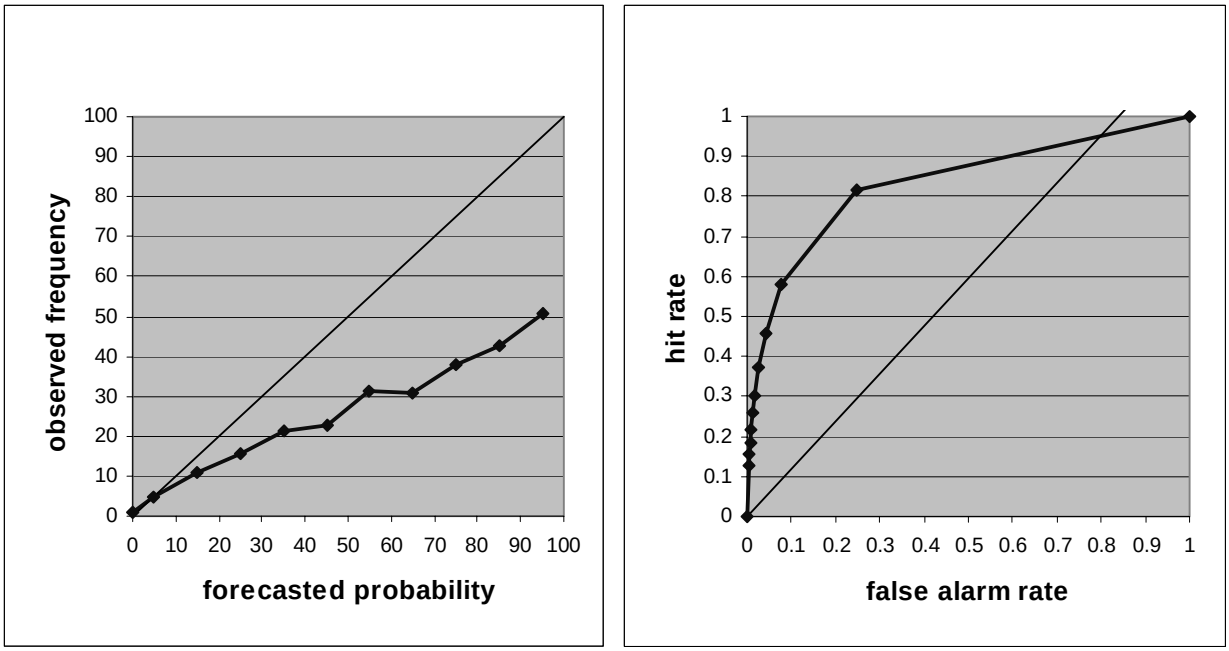

Figure 9: Reliability diagram (left) and ROC (right) for the forecast probability that a TC will pass within 65 nm anytime during the first 120 hours of the forecast; each point on the ROC corresponds to a different threshold: from top-right to bottom-left these are 0%, >0%, >10%, >20%, …, >90% and 100%

In order to demonstrate the benefit of a statistical approach in the medium forecast range compared to a purely deterministic one, a thorough evaluation between the two is needed. The ROC curves presented in Fig. 6 and Fig. 9 are based on the probabilistic approach, each point representing a different probability threshold for the event. ROC diagrams can also be made for a deterministic approach. By varying the

definition of the event itself, one can generate different contingency tables, each one representing a point on the ROC curve.

5 Future developments

The production and evaluation of TC tracks and strike probability will continue routinely. Strike probability maps will soon become available on the ECMWF web server with access restricted to ECMWF Member States at first. There are plans to make the strike probability images on the web and the track forecasts in BUFR on the GTS available to WMO RSMC's with a responsibility for tropical cyclone warnings.

Acknowledgements

Thanks to Horst Böttger, François Lalaurette and Martin Miller for their comments on the manuscript. Special thanks to Hans Hersbach for providing the sub-grid interpolation scheme (see appendix) and Mike Fiorino for making the "enhanced FNMOC tracker" software available as a means for validating the ECMWF TC tracker.

References

Barkmeijer, J., Buizza, R., Palmer, T.N., Puri, K., and J.-F. Mahfouf, 2001: Tropical singular vectors computed with linearized diabatic physics. *Quart. J. Roy. Met. Soc.*, **127**, 685-708.

Buizza, R., 1997: Potential forecast skill of ensemble prediction and spread and skill distributions of the ECMWF ensemble prediction system. *Mon. Wea. Rev.*, **125**, 99-119.

Elsberry, R.L., and L.E. Carr III, 2000: Consensus of dynamical tropical cyclone track forecasts - Errors versus spread. *Mon. Wea. Rev.*, **128**, 4131-4138.

Dong, K., and C.J. Neumann, 1983: On the relative motion of binary tropical cyclones. *Mon. Wea. Rev.*, **111**, 945-953.

Fiorino, M., 2002: SHEM 2001-2002 global model tropical cyclone forecasts. http://metoc.npmoc.navy.mil/jtwc/sitrep/2002.shem/

Heming, J., 1994: Keeping on eye on the hurricane - Verification of tropical cyclone forecast tracks at the Met. Office. *NWP Gazette*, **1**, 2-8.

Marchok, T.P., 2002: How the NCEP tropical cyclone tracker works. *Preprints*, 25th conference on hurricanes and tropical meteorology, San Diego, CA, 21-22.

Palmer, T.N., Barkmeijer, J., Buizza, R., Jakob, C., Lalaurette, F., Paccagnella, T., and D. Richardson, 2001: Severe weather prediction. *ECMWF Tech. Memo.*, **352**.

Puri, K., Barkmeijer, J. and T.N. Palmer, 2001: Ensemble prediction of tropical cyclones using targeted diabatic singular vectors. *Quart. J. Roy. Met. Soc.*, **127**, 709-731.

U.K. Met. Office, 2001: http://www.metoffice.gov.uk/sec2/sec2cyclone/tcbulletins/2001/September.html

Sinclair, M.R., 1994: An objective cyclone climatology study for the southern hemisphere. *Mon. Wea. Rev.*, **122**, 2239-2256.

Vitart, F., Stockdale, T.N., 2001: Seasonal forecasting of tropical storms using coupled GCM integrations. *Mon. Wea. Rev.*, **129**, 2521-2537.

Appendix: Estimation of a sub-grid minimum from a gridded field

Assume a field (e.g. mean sea level pressure) $p(\mathrm{r}_{ij})$, defined at grid locations r_{ij}. The way in which r is parameterised (lat-lon in degrees, km,…,) is in principle irrelevant.

Question: At what sub-grid location r_0 *is p expected to have its minimum* p_0 *?*

Let *p*, constrained to grid locations, be minimal at $\mathrm{r}_m; p_m \equiv p(\mathrm{r}_m)$. Let the values of *p* at its four nearest grid points $\mathrm{r}_{m\pm\Delta_{1,2}}$ be given by $p_{m\pm\Delta_{1,2}}$, where $\Delta_{1,2}$ is the grid spacing in direction (1,2), e.g. lat-lon in degrees or km.

If one assumes that *p* is locally quadratic around its minimum for a range of at least two grid distances $\Delta_{1,2}$, and if one neglects the effects of the earth's curvature then:

$$p(\mathrm{r}) \approx p_0 + (\mathrm{r}-\mathrm{r}_0)A(\mathrm{r}-\mathrm{r}_0), \tag{1}$$

for $\mathrm{r}=\mathrm{r}_m$ and $\mathrm{r}=\mathrm{r}_{m\pm\Delta_{1,2}}$, where

$$A=\begin{pmatrix} a_1 & b \\ b & a_2 \end{pmatrix}. \tag{2}$$

This defines 5 equations for 6 unknowns: a position r_0 (2), A minimum p_0 (1) and a matrix *A* (3). Neglecting the effect caused by the difference of the normal axes of the minimum from the N-S and E-W direction, then *b* may be set to zero and a unique solution to the set of 5 equations can be found (otherwise, next-nearest grid points need to be taken into consideration as well). Let

$$d_{1,2} = p_{m+\Delta_{1,2}} - p_{m-\Delta_{1,2}}, \tag{3}$$

$$s_{1,2} = p_{m+\Delta_{1,2}} + p_{m-\Delta_{1,2}} - 2p_m, \tag{4}$$

then it is straightforward to show that the minimum p_0 and position r_0 are given by:

$$p_0 = p_m - \frac{1}{8}\sum_{i=1}^{2}\frac{d_i^2}{s_i} \tag{5}$$

$$(\mathrm{r}_0)_i = (\mathrm{r}_m)_i - \frac{1}{2}\Delta_i\frac{d_i}{s_i} \tag{6}$$

Remarks:

Because p_m is the gridded minimum, $s_{1,2} \geq 0$.. In case $s_i = 0, p$ is either constant in direction *i* or contains more than one local minimum.

It is easy to show that $|d_i/s_i| \leq 1$. Therefore, p_0 is always within half a grid box distance from the gridded minimum position p_m.